JJCO Japanese Journal of Clinical Oncology

Jpn J Clin Oncol 2010;40(8)788–794
doi:10.1093/jjco/hyq044
Advance Access Publication 20 April 2010

Clinical Outcomes of Stereotactic Brain and/or Body Radiotherapy for Patients with Oligometastatic Lesions

Tetsuya Inoue[1,*], Norio Katoh[1], Hidefumi Aoyama[1], Rikiya Onimaru[1], Hiroshi Taguchi[1], Shunsuke Onodera[1], Satoshi Yamaguchi[2] and Hiroki Shirato[1]

[1]Department of Radiology, Hokkaido University Graduate School of Medicine and [2]Department of Medical Physics, Hokkaido University Graduate School of Medicine, Sapporo, Japan

*For reprints and all correspondence: Tetsuya Inoue, Department of Radiology, Hokkaido University Graduate School of Medicine, North 15 West 7, Kita-ku, Sapporo 060-8638, Japan. E-mail: t-inoue@med.hokudai.ac.jp

Received November 30, 2009; accepted March 11, 2010

Objective: Several recent studies have shown that oligometastatic disease has curative potential, although it was previously considered to signal a patient's last stage of life. Stereotactic body radiotherapy has been available for extra-cranial metastases in addition to stereotactic cranial radiotherapy for brain metastases. The aim of the present study was to retrospectively evaluate the clinical outcomes of stereotactic radiotherapy for patients with oligometastatic lesions.

Methods: Between 1999 and 2008, 41 patients with five or fewer detectable metastases were treated with stereotactic radiotherapy at our institution. The treated oligometastatic lesions were in the brain, lung and adrenal glands.

Results: With a median follow-up period of 20 months, the 3-year overall survival, progression-free survival, local control and distant control rates were 39%, 20%, 80% and 35%, respectively, and the respective 5-year rates were 28%, 20%, 80% and 35%. The median survival time was 24 months. According to interval to recurrence, the 3- and 5-year overall survival rates were 19% and 10%, respectively, for patients with <12 months ($n=18$), compared with 53% and 40% for those with ≥ 12 months ($n=23$) ($P=0.006$).

Conclusions: Precise stereotactic radiotherapy was effective in controlling oligometastatic lesions for patients with a median survival time of 24 months. Interval to recurrence may impact the overall survival rate and should be included in the stratification criteria in a prospective randomized trial to investigate the benefits of stereotactic radiotherapy for patients with oligometastases.

Key words: oligometastases – stereotactic body radiotherapy – stereotactic radiotherapy – radiosurgery

INTRODUCTION

Most patients who have had any recurrent or metastatic sites of cancer are considered to be in their last stage of life. However, stereotactic cranial radiosurgery (SCRS) and stereotactic cranial radiotherapy (SCRT) have been shown to be useful for prolonging useful life in patients with solitary or oligo brain metastases with or without whole brain radiotherapy (WBRT) (1,2). The treatment outcomes are related to the number of metastases and the presence or absence of extra-cranial disease (3). A Phase III study has suggested that SCRS with WBRT results in better survival than WBRT alone for patients with a single brain metastasis or patients with tumors > 2.0 cm in diameter (4). These studies have shed light on the possibility of improving treatment outcomes by using high-dose local radiotherapy with or without whole-body cancer treatment in patients with extra-cranial metastasis.

Stereotactic body radiotherapy (SBRT) with high local dose has been applied to extra-cranial diseases such as peripheral Stage I non-small cell lung cancer (NSCLC) and has been reported to provide excellent local control (LC) and survival compatible with surgery (5,6). Recently, indications for SBRT have been extended to include lung metastases (7–9), liver metastases (10,11), adrenal gland metastases (12,13), spinal metastases (14–16), and others (17). Excellent LC has been reported in these reports, but the clinical benefits of SBRT for extra-cranial metastasis are yet to be determined. In most of these studies, SBRT was used for patients with fewer than five metastatic sites or for those in the clinical state of so-called oligometastasis (18).

The clinical state of oligometastatic disease was proposed in 1995 by Hellman and Weichselbaum (18), who hypothesized that LC of oligometastases may yield improved systemic control and prolonged survival. Niibe et al. (19–21) have also reported the state of oligometastasis/oligo-recurrence. They suggested that some oligometastasis/oligo-recurrence patients could survive for as long as the patients with primary cancer only, and thus these patients must be treated curatively. Improvements in diagnostic modalities have facilitated early detection of small metastatic lesions, both intra-cranial and extra-cranial, and have provided a sound rationale for Hellman and Weichselbaum's hypothesis. Recent clinical research has shown that some patients with recurrence or distant metastases can expect long-term survival after SBRT and SCRT (7–11,19–23). It remains uncertain whether these results are due to selection bias or some positive effect of SBRT and SCRT. A prospective randomized trial should be undertaken to answer this question, but prognostic factors to stratify the patients are not yet well understood.

In this study, we retrospectively analyzed our experience with SBRT and/or SCRT/SCRS for patients with oligometastases.

PATIENTS AND METHODS

Patient Characteristics

A database of patients who received SBRT and SCRT/SCRS at our institution was used to select the patients whose primary sites were treated by surgery or definitive radiation therapy between 1995 and 2007. There were 41 patients who had five or fewer detectable oligometastatic lesions at the time of SBRT and/or SCRT and had been treated with SBRT and/or SCRT/SCRS between 1999 and 2008. Diagnosis of the oligometastatic lesions was based on whole-body computed tomography (CT) and brain magnetic resonance imaging (MRI) findings. Fluorodeoxyglucose-positron emission tomography was performed as needed. The oligometastatic lesions were diagnosed by diagnostic radiologists during the diagnostic evaluation.

The treatment methods for the primary sites were surgery in 23 patients and definitive radiotherapy in 18. Definitive radiotherapy consisted of conventional radiotherapy in 8 patients and SBRT in 10.

There were seven patients who had previously been treated by SBRT and/or SCRT/SCRS to oligometastatic sites prior to receiving surgery or radiotherapy at their primary sites. The treatment time interval between the surgery/definitive radiation therapy to the primary sites and the initial SBRT and/or SCRT/SCRS to oligometastatic sites ranged from 1 to 4 months (median 2 months) in these seven patients. In the other 34 patients, the median treatment interval time from primary sites to oligometastatic sites was 21 months (range 0–121 months). We defined the treatment interval time from primary sites to oligometastatic sites as interval to recurrence. In this study, all analyses started from the day of SBRT and/or SCRT/SCRS to oligometastatic sites.

The patient characteristics are given in Table 1. There were 22 men and 19 women, and the median age was 66 years (range 30–82 years). The primary cancers consisted of lung cancer, head and neck cancer, breast cancer, colorectal cancer, renal cell carcinoma, renal pelvic cancer, hepatocellular carcinoma, thymic cancer and apocrine gland cancer. The study patients were separated into a favorable group (breast, colorectal, renal, thymic and apocrine gland cancer) and others, according to Rusthoven et al. (10). The primary histology was mainly adenocarcinoma. The number of oligometastatic tumors was mainly one or two tumors; there were only two patients who had three oligometastatic tumors and only one patient who had five. The sites involved with the oligometastatic lesions were the brain, lung and adrenal gland. Lung and adrenal gland metastases were treated by SBRT. There were no patients with oligometastatic liver metastases treated by SBRT at our institution. Fourteen patients were treated by chemotherapy as an adjuvant therapy or as a treatment for recurrence or metastases. No chemotherapy was administered during the treatment for oligometastases. No patients underwent surgical removal of the metastatic lesions.

There were 24 patients who had single or multiple brain metastases. Brain metastases were treated by SCRT or SCRS. According to the recursive partitioning analysis, 5, 18 and 1 patients were classified as Class I, Class II and Class III, respectively.

SCRT/SCRS Technique

Fifteen of 24 patients were treated by SCRT alone, five by SCRS alone and four by SCRS with WBRT for their brain metastases. The patients who received WBRT were randomly assigned to the group of SCRS with WBRT by the clinical trial of the Japanese Radiation Oncology Study Group (JROSG 99-1) (2). These patients were treated with 6- or 10-MV photons using a linac-based stereotactic system and were immobilized by a thermoshell in SCRT and a stereotactic frame in SCRS. The gross tumor volume (GTV) was defined based on MRI and CT images. A 1–3-mm

Table 1. Patient characteristics (41 patients)

Characteristics	Value
Age (years)	
Median	66
Range	30–82
Gender (*n*)	
Male	22
Female	19
Primary cancer (*n*)	
Lung	25
Head and neck	6
Breast	3
Colorectal	2
Liver	1
Renal	1
Renal pelvic	1
Thymic	1
Apocrine gland	1
Primary histology (*n*)	
Adenocarcinoma	23
Squamous cell carcinoma	6
Thyroid cancer	2
Large cell carcinoma	2
Others	8
Treatment for primary cancer (*n*)	
Resection	23
SBRT	10
Conventional radiation therapy	8
Sites involved with oligometastatic disease (no. of tumors)	
Brain	33
Lung	22
Adrenal gland	5
Number of oligometastatic tumors (*n*)	
1	27
2	11
3	2
4	0
5	1
Number of oligometastatic involved organs (*n*)	
1	37
2	4

SBRT, stereotactic body radiotherapy.

margin was added to the GTV to create the planning target volume (PTV). Treatment was prescribed to the 100% isodose line, with the 80–90% isodose line covering the PTV. A total dose of 15–25 Gy was administered in one fraction for SCRS, and a total dose of 20–40 Gy was administered in four fractions for SCRT. A total dose of 30 Gy was administered in 10 fractions for WBRT.

SBRT Technique

All patients with lung metastases and 10 patients with primary lung cancer received SBRT as the definitive radiotherapy. They received real-time tumor-tracking radiotherapy (RTRT). The RTRT system has been described in detail elsewhere (24,25). In brief, 1.5–2.0-mm gold markers were implanted near the tumor by means of image-guided procedures. CT scans were taken with the patients holding their breath at the end of normal expiration. The GTV was contoured in axial CT images. The clinical target volume (CTV) was defined three dimensionally as the GTV on CT with a 6–8-mm margin for primary lung cancers and was considered to be equal to the internal target volume. We treated adrenal gland metastases using the RTRT system. The CTV was defined as the GTV on CT with a 3-mm margin for adrenal gland metastases and with a 5-mm margin for lung metastases. The PTV was three dimensionally defined as the CTV plus a 5-mm margin with optimal reduction near the organ at risk.

Treatment was prescribed to the 100% isodose line covering the PTV within the 80% isodose line. Patients were treated with 4-, 6- or 10-MV photons. SBRT was delivered by using multiple non-coplanar static ports. A total dose of 48 Gy was administered in eight fractions in patients with adrenal gland metastases. A total dose of 35–60 Gy was administered in four or eight fractions in patients with lung metastases or primary lung cancer, respectively.

Statistical Analysis

LC was defined as no progression of the tumor in the CTV, and marginal recurrence was counted as local failure in this study. Follow-up of the patients was based on clinical examination in the outpatient clinic and/or periodic radiological examination. In principle, radiological examinations such as chest X-ray, whole-body CT and brain MRI were performed once every 3–4 months, but the frequency strongly depended on the clinical situation. The overall survival (OS) and progression-free survival (PFS) rates were calculated from the day of SBRT and/or SCRT/SCRS to oligometastatic sites using the Kaplan–Meier method.

Possible prognostic factors were as follows: age, gender, primary cancer, primary histology, treatment for primary cancer, sites involved with oligometastatic disease, number of oligometastatic tumors and the treatment interval time from primary sites to oligometastatic sites (defined as interval to recurrence). The log-rank test was used to calculate the statistically significant differences. A value of $P < 0.05$ was considered to be statistically significant. Significant variables on univariate analysis (UVA) were tested with

multivariate analyses (MVA). MVA was performed using a Cox proportional hazards regression model.

RESULTS

Local Tumor Response and Distant Metastases

The median follow-up period was 20 months (range 1–111 months). The 3- and 5-year LC rates were each 80%, and the 3- and 5-year distant control (DC) rates were each 35% (Fig. 1).

Survival

The 3-year OS and PFS rates were 39% and 20%, respectively; and the respective 5-year rates were 28% and 20% (Fig. 2). The median survival time (MST) was 24 months. Patients with adrenal gland metastasis had an MST of 15 months.

Age, primary histology and the number of oligometastatic tumors were not found to be statistically significant prognostic factors for the OS rate; however, gender, primary cancer, treatment for primary cancer, oligometastatic lung disease and interval to recurrence were statistically significant prognostic factors for the OS rate in the UVA shown in Table 2.

The OS of female patients was significantly longer than that of male patients ($P = 0.01$), and the OS of patients who had undergone resection for primary cancer was significantly longer than those of others ($P = 0.0006$). For patients with primary cancer from favorable primary sites ($n = 8$), the 3- and 5-year OS rates were both 86%, compared with 27% and 17%, respectively, for patients with primary cancer from other primary sites ($n = 33$, $P = 0.02$). We separated the patients into two groups according to interval to recurrence of <12 or ≥ 12 months ($n = 18$, 23, respectively). The 3- and 5-year OS rates were 19% and 10%, respectively, for those with an interval to recurrence of <12 months, compared with 53% and 40%, respectively, for those with an interval to recurrence of ≥ 12 months (Fig. 3; $P = 0.006$). For patients with oligometastatic lung disease with or without brain/adrenal metastases ($n = 16$), the 3- and 5-year OS rates were both 63%, compared with 22% and 14%, respectively, for patients with only brain/adrenal metastases ($n = 25$) (Fig. 4; $P = 0.009$). MVA showed no statistically significant prognostic factors for the OS rate.

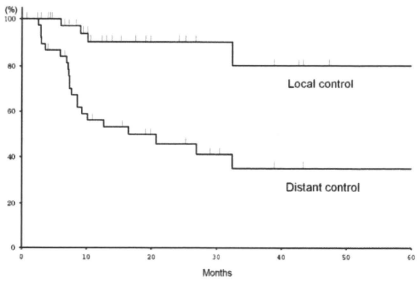

Figure 1. Kaplan–Meier actuarial local control and distant control rate.

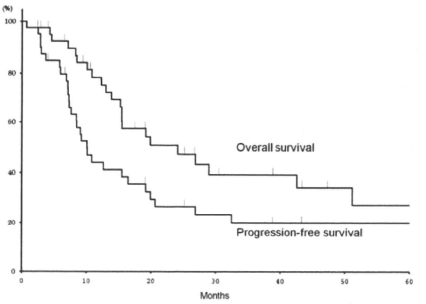

Figure 2. Kaplan–Meier actuarial overall survival (OS) and progression-free survival rate.

Table 2. UVA and MVA for OS rate

Variables	*P* value	
	UVA	MVA
Age		
<65 years	0.72	
Gender		
Female[a]	0.01*	0.72
Primary cancer		
Favorable[a]	0.02*	0.37
Primary histology		
Adenocarcinoma	0.84	
Treatment for primary cancer		
Resection[a]	0.0006*	0.26
Sites involved with oligometastatic disease		
Brain	0.09	
Lung	0.009*	0.47
Adrenal gland	0.09	
Number of oligometastatic tumors		
Single metastasis	0.47	
Interval to recurrence		
≥12 months[a]	0.006*	0.52

UVA, univariate analysis; MVA, multivariate analysis; OS, overall survival.
*Significant ($P < 0.05$).
[a]These variables were favorable predictors for overall survival rate on UVA.

Long Survivors

Four 5-year survivors consisted of two with lung adenocarcinoma, one with renal pelvic cancer and one with thymic cancer. One patient with lung adenocarcinoma had one brain metastasis treated by SCRT, whereas the other patient with lung adenocarcinoma had one brain metastasis treated by SCRS with WBRT and one lung metastasis treated by SBRT. The patient with renal pelvic cancer had two lung metastases treated by SBRT, and the patient with thymic cancer had one lung metastasis treated by SBRT.

Toxicities

Adverse effects were graded according to the Common Toxicity Criteria for Adverse Events, version 3.0. Grade 2 complications occurred in four patients (9.8%), radiation necrosis of the brain occurred in three patients and intercostal neuralgia occurred in one patient. No other adverse effects of Grade 2 or more were observed.

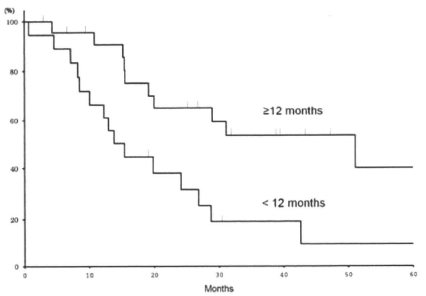

Figure 3. Kaplan–Meier curve of OS rates for patients with interval to recurrence of <12 months ($n = 18$) and ≥12 months ($n = 23$). Significant statistical difference was found ($P = 0.006$) between the two groups.

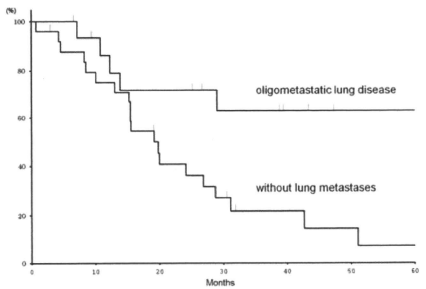

Figure 4. Kaplan–Meier curve of OS rates for patients with oligometastatic lung disease with or without brain/adrenal metastases ($n = 16$) and only brain/adrenal metastases ($n = 25$). Significant statistical difference was found ($P = 0.009$) between the two groups.

DISCUSSION

In this study, the OS rates at 3 and 5 years were 39% and 28%, respectively, and the MST was 24 months, which is equivalent to that in the study of oligometastases previously published, as follows. Milano et al. (22) reported the results of a Phase II trial using SBRT to a dose of 50 Gy in 10 fractions in the treatment of oligometastatic disease with 4-year OS, PFS, LC and DC rates of 28%, 20%, 60% and 25%, respectively. Patients with breast cancer fared significantly better with respect to OS, PFS, LC and DC rates (26), and those with adrenal metastases had significantly worse OS, LC and DC rates (13).

Rusthoven et al. (9,10) have recently reported the results of multi-institutional Phase I/II trials of SBRT for lung and liver metastases. The actual LC rate at 1 and 2 years after SBRT for oligometastatic lung tumors were 100% and 96%, respectively, and the MST was 19 months. The actual in-field LC rates at 1 and 2 years after SBRT for oligometastatic liver tumors were 95% and 92%, respectively, and the MST was 20.5 months. The primary tumor site was significantly predictive of survival. Primary tumors of the lung and ovary as well as non-colorectal gastrointestinal malignancies were found to be associated with poorer survival compared with breast, colorectal, renal, carcinoid and gastrointestinal stromal tumors as well as sarcoma.

Flannery et al. (23) have reported long-term survival in patients with synchronous solitary brain metastasis from NSCLC treated with radiosurgery. The MST was 18 months, and the 1-, 2- and 5-year actuarial OS rates were 71.3%, 34.1% and 21%, respectively. For patients who underwent definitive thoracic therapy, the 5-year actuarial OS rate was 34.6% compared with 0% for those who had non-definitive therapy. The Karnofsky performance status (KPS) also significantly impacted the OS rate.

SBRT and SCRT have been applied for the treatment of metastatic lesions recently; however, conventional radiotherapy remains a standard option for the treatment of metastatic lesions. Andrews et al. (4) reported the result of a Phase III study that compared WBRT with or without SCRS for brain metastases. This study showed WBRT with SCRS improved survival for patients with single brain metastasis or patients with tumors > 2.0 cm in diameter. To our knowledge, there has been no study that compared SBRT with conventional radiotherapy for extra-cranial metastases.

It is important to find prognostic factors related to long-term survival after definitive therapy such as SBRT and SCRT for oligometastatic lesions. According to the studies described above, KPS, the primary tumor site and the oligometastatic site can be predictive of survival. Low KPS, a primary tumor site such as the lung and adrenal metastasis were found to be associated with lower survival in the

previous study (9,10,13,22,23,26). However, our results have shown that some patients with lung cancer can survive >5 years after treatment for oligometastases and that some with adrenal metastatic tumors can expect an MST of 15 months. These findings are consistent with those of Khan et al. (27). It would therefore be useful to find prognostic factors that are independent of the primary and metastatic sites.

In this study, we identified another factor that can be used to predict long-term survival. The treatment interval time from primary sites to oligometastatic sites, defined as interval to recurrence, was found to be significantly associated with the OS rate in the UVA. A long interval to recurrence implies that the patient has a slowly growing tumor or is under good control with regard to primary and other sites except for the apparent metastatic lesions. In contrast, a short interval to recurrence indicates rapid tumor growth or poor control of the primary and other metastatic sites. Although it was difficult to distinguish between the natural course of the disease and the effects of treatment in this retrospective study, interval to recurrence was shown to be an independent parameter to predict prognosis for patients with oligometastases.

The clinical state of oligometastatic disease was proposed in 1995 by Hellman and Weichselbaum (18), but a clear definition for oligometastasis has not yet been established. Table 3 shows various definitions of oligometastasis reported previously in the literature. The number of oligometastases ranges from 1 to 6 tumors. Oligometastatic lesions are mainly in the lung, liver and brain, although oligometastases in the bone, adrenal gland, lymphatic nodes and soft tissue have also been reported. In the present study, we defined the number of oligometastases as ranging from 1 to 5 tumors, and oligometastatic lesions were found in the lung, brain and adrenal gland, which is consistent with several previous reports. A definitive definition of oligometastasis may not be possible, due to its diverse nature, but a clear definition is required for further investigation.

Table 3. Definition of oligometastasis

	Number of patients	Oligometastases	Oligometastatic lesions
Norihisa et al. (8)	34	1–2	Lung
Rusthoven et al. (9)	38	1–3	Lung
Rusthoven et al. (10)	47	1–3	Liver
Katz et al. (11)	69	1–6	Liver
Rades et al. (14)	521	1–3	Vertebrae
Salama et al. (17)	29	1–5	Lung, node, liver, bone, soft tissue, adrenal gland
Milano et al. (22)	121	1–5	Lung, node, liver, brain, adrenal gland, bone
Flannery et al. (23)	42	1	Brain
Khan et al. (27)	23	1–2	Lung, brain, soft tissue, adrenal gland, bone
Current study	41	1–5	Lung, brain, adrenal gland

One shortcoming of this paper is the retrospective nature of the analysis. Patients with sufficient medical conditions were probably selected beforehand to receive SBRT and SCRT. The large number of patients who died within a short period may have masked the possible progression of the disease and local failure. However, it is notable that there is a definite group of patients treated with SBRT and SCRT who experienced long survival even with distant metastasis. A large prospective trial is required to investigate the actual benefits of SBRT and SCRT for patients with oligometastases. Our findings suggest that interval to recurrence should be included in the stratification criteria in a prospective randomized trial comparing treatment with or without SBRT and SCRT.

In conclusion, precise SBRT and SCRT were effective in controlling oligometastatic lesions for patients with an MST of 24 months. Interval to recurrence may impact the OS rate and should be included in the stratification criteria of a prospective randomized trial to investigate the benefits of SBRT and SCRT for patients with oligometastases.

Conflict of interest statement

None declared.

References

1. Aoyama H, Shirato H, Onimaru R, Kagei K, Ikeda J, Ishii N, et al. Hypofractionated stereotactic radiotherapy alone without whole-brain irradiation for patients with solitary and oligo brain metastasis using noninvasive fixation of the skull. *Int J Radiat Oncol Biol Phys* 2003;56:793–800.
2. Aoyama H, Shirato H, Tago M, Nakagawa K, Toyoda T, Hatano K, et al. Stereotactic radiosurgery plus whole-brain radiation therapy vs stereotactic radiosurgery alone for treatment of brain metastases: a randomized controlled trial. *JAMA* 2006;295:2483–91.
3. Sperduto PW, Berkey B, Gaspar LE, Mehta MCurran W. A new prognostic index and comparison to three other indices for patients with brain metastases: an analysis of 1960 patients in the RTOG database. *Int J Radiat Oncol Biol Phys* 2008;70:510–4.
4. Andrews DW, Scott CB, Sperduto PW, Flanders AE, Gaspar LE, Schell MC, et al. Whole brain radiation therapy with or without stereotactic radiosurgery boost for patients with one to three brain metastases: phase III results of the RTOG 9508 randomised trial. *Lancet* 2004;3:1665–72.
5. Onishi H, Shirato H, Nagata Y, Hiraoka M, Fujino M, Gomi K, et al. Hypofractionated stereotactic radiotherapy (HypoFXSRT) for stage I non-small cell lung cancer: updated results of 257 patients in a Japanese multi-institutional study. *J Thorac Oncol* 2007;2:S94–100.
6. Baumann P, Nyman J, Hoyer M, Wennberg B, Gagliardi G, Lax I, et al. Outcome in a prospective phase II trial of medically inoperable stage I non-small-cell lung cancer patients treated with stereotactic body radiotherapy. *J Clin Oncol* 2009;20:3290–6.
7. Okunieff P, Petersen AL, Philip A, Milano MT, Katz AW, Boros L, et al. Stereotactic body radiation therapy (SBRT) for lung metastases. *Acta Oncol* 2006;45:808–17.

8. Norihisa Y, Nagata Y, Takayama K, Matsuo Y, Sakamoto T, Sakamoto M, et al. Stereotactic body radiotherapy for oligometastatic lung tumors. *Int J Radiat Oncol Biol Phys* 2008;72:398–403.
9. Rusthoven KE, Kavanagh BD, Burri SH, Chen C, Cardenes H, Chidel MA, et al. Multi-institutional phase I/II trial of stereotactic body radiation therapy for lung metastases. *J Clin Oncol* 2009;27:1579–84.
10. Rusthoven KE, Kavanagh BD, Cardenes H, Stieber VW, Burri SH, Feigenberg SJ, et al. Multi-institutional phase I/II trial of stereotactic body radiation therapy for liver metastases. *J Clin Oncol* 2009;27:1572–8.
11. Katz AW, Carey-Sampson M, Muhs AG, Milano MT, Schell MC, Okunieff P. Hypofractionated stereotactic body radiation therapy (SBRT) for limited hepatic metastases. *Int J Radiat Oncol Biol Phys* 2007;67:793–8.
12. Katoh N, Onimaru R, Sakuhara Y, Abo D, Shimizu S, Taguchi H, et al. Real-time tumor-tracking radiotherapy for adrenal tumors. *Radiother Oncol* 2008;87:418–24.
13. Chawla S, Chen Y, Katz AW, Muhs AG, Philip A, Okunieff P, et al. Stereotactic body radiotherapy for treatment of adrenal metastases. *Int J Radiat Oncol Biol Phys* 2009;75:71–5.
14. Rades D, Veninga T, Stalpers LJ, Basic H, Rudat V, Karstens JH, et al. Outcome after radiotherapy alone for metastatic spinal cord compression in patients with oligometastases. *J Clin Oncol* 2007;25:50–6.
15. Yamada Y, Bilsky MH, Lovelock DM, Venkatraman ES, Toner S, Johnson J, et al. High-dose, single-fraction image-guided intensity-modulated radiotherapy for metastatic spinal lesions. *Int J Radiat Oncol Biol Phys* 2008;71:484–90.
16. Sahgal A, Ames C, Chou D, Ma L, Huang K, Xu W, et al. Stereotactic body radiotherapy is effective salvage therapy for patients with prior radiation of spinal metastases. *Int J Radiat Oncol Biol Phys* 2009;74:723–31.
17. Salama JK, Chmura SJ, Mehta N, Yenice KM, Stadler WM, Vokes EE, et al. An initial report of a radiation dose-escalation trial in patients with one to five sites of metastatic disease. *Clin Can Res* 2008;14:5255–9.
18. Hellman S, Weichselbaum RR. Oligometastases. *J Clin Oncol* 1995;13:8–10.
19. Niibe Y, Kazumoto T, Toita T, Yamazaki H, Higuchi K, Ii N, et al. Frequency and characteristics of isolated para-aortic lymph node recurrence in patients with uterine cervical carcinoma in Japan: a multi-institutional study. *Gynecol Oncol* 2006;103:435–8.
20. Niibe Y, Kenjo M, Kazumoto T, Michimoto K, Takayama M, Yamauchi C, et al. Multi-institutional study of radiation therapy for isolated para-aortic lymph node recurrence in uterine cervical carcinoma: 84 subjects of a population of more than 5,000. *Int J Radiat Oncol Biol Phys* 2006;66:1366–9.
21. Niibe Y, Kuranami M, Matsunaga K, Takaya M, Kakita S, Hara T, et al. Value of high-dose radiation therapy for isolated osseous metastasis in breast cancer in terms of oligo-recurrence. *Anticancer Res* 2008;28:3929–31.
22. Milano MT, Katz AW, Muhs AG, Philip A, Buchholz DJ, Schell MC, et al. A prospective pilot study of curative-intent stereotactic body radiation therapy in patients with 5 or fewer oligometastatic lesions. *Cancer* 2008;112:650–8.
23. Flannery TW, Suntharalingam M, Regine WF, Chin LS, Krasna MJ, Shehata MK, et al. Long-term survival in patients with synchronous, solitary brain metastasis from non-small-cell lung cancer treated with radiosurgery. *Int J Radiat Oncol Biol Phys* 2008;72:19–23.
24. Shirato H, Shimizu S, Kunieda T, Kitamura K, van Herk M, Kagei K, et al. Physical aspects of a real-time tumor-tracking system for gated radiotherapy. *Int J Radiat Oncol Biol Phys* 2000;48:1187–95.
25. Shirato H, Shimizu S, Kitamura K, Nishioka T, Kagei K, Hashimoto S, et al. Four-dimensional treatment planning and fluoroscopic real-time tumor tracking radiotherapy for moving tumor. *Int J Radiat Oncol Biol Phys* 2000;48:435–42.
26. Milano MT, Zhang H, Metcalfe SK, Muhs AG, Okunieff P. Oligometastatic breast cancer treated with curative-intent stereotactic body radiation therapy. *Breast Cancer Res Treat* 2009;115:601–8.
27. Khan AJ, Mehta PS, Zusag TW, Bonomi PD, Penfield Faber L, Shott S, et al. Long term disease-free survival resulting from combined modality management of patients presenting with oligometastatic, non-small cell lung carcinoma (NSCLC). *Radiother Oncol* 2006;81:163–7.

Original Article | DOI 10.3349/ymj.2010.51.4.557 pISSN: 0513-5796, eISSN: 1976-2437 | Yonsei Med J 51(4):557-561, 2010 | YMJ

Cesium Implant for Tongue Carcinoma with a Thickness of 1.5 cm or More: Cases Successfully Treated with a Modified Manchester System

Takeshi Nishioka,[1] Masaharu Fujino,[2] Akihiro Homma,[3] Tetsuro Yamashita,[2] Akira Sato,[4] Keiichi Ohmori,[5] Kenichi Obinata,[5] Hiroki Shirato,[6] Kenichi Notani,[4] and Masamichi Nishio[7]

[1]Department of Biomedical Sciences and Engineering, Faculty of Health Sciences, Graduate School of Health Sciences, Hokkaido University, Sapporo; [2]Department of Oral Surgery, Keiyukai Sapporo Hospital, Sapporo; [3]Department of Otolaryngology, Head and Neck Surgery, Hokkaido University Graduate School of Medicine, Sapporo; [4]Oral Diagnosis and Medicine, Graduate School of Dental Medicine, Hokkaido University, Sapporo; [5]Department of Dental Radiology, Graduate School of Dental Medicine, Hokkaido University Hospital, Sapporo; [6]Department of Radiology, Graduate School of Medicine, Hokkaido University, Sapporo; [7]Department of Radiology, Hokkaido Cancer Centre, Sapporo, Japan.

Reveived: June 4, 2009
Revised: September 7, 2009
Accepted: September 11, 2009
Corresponding author: Dr. Takeshi Nishioka, Department of Biomedical Sciences and Engineering, Faculty of Health Sciences, Graduate School of Health Sciences, Hokkaido University, N12W5 Kita-ku, Sapporo 064-0812, Japan.
Tel: 81-11-706-3411, Fax: 81-11-706-3411
E-mail: trout@hs.hokudai.ac.jp

· The authors have no financial conflicts of interest.

Purpose: Deciding on treatment carcinoma of the tongue when the tumor has a thickness of 1.5 cm or more is difficult. Surgery often requires wide resection and re-construction, leading to considerable functional impairment. A cesium implant is an attractive option, but according to the Manchester System, a two plane implant is needed. **Materials and Methods:** According to the textbook, a tumor is sandwiched between the needles, which are implanted at the edge of the tumor. This may cause an unnecessarily high dose to the outer surface of the tongue, which sometimes leads to a persistent ulcer. To avoid this complication, we invented a modified implantation method, and applied the method to five consecutive patients. **Results:** With a minimum follow-up of 2 years, all primary tumors in 5 consecutive patients have been controlled. No complications occurred in soft tissue of the tongue or in the mandible. **Conclusion:** Our modified Manchester System was feasible and effective for tumors that has a thickness of 1.5 cm or more.

Key Words: Carcinoma of the tongue, brachytherapy, cesium, neck dissection

INTRODUCTION

Carcinoma of the mobile tongue can be successfully treated by surgery or radiotherapy provided that the tumor is small, typically with a thickness less than or equal to 1.2 cm.[1] We have been using the Manchester System for the past 3 decades, although sometimes external radiation was also combined with cesium (Cs) brachytherapy. Hosokawa, et al.[2] has reported on the treatment results of combination therapy at our institute. The percent of patients with 5 year local control for T1 and T2 diseases were 92.6% and 62.7%, respectively.[2] The value for T1 disease was comparable with the results achieved at other institutions. However, the T2 control rate was far from satisfactory, and therefore, in 1993, we changed the treatment protocol from combination therapy to brachytherapy alone (7000 cGy). Since then, the 3 year local control rates obtained for T2 disease was

88% (unpublished data). Compared to T1 disease, T2 disease covers a wide range of diseases; the horizontal and vertical lengths vary from 2 to 4 cm, and thickness is sometimes ambiguous. Among these characteristics, tumor thickness is the major concern when treatment policy is discussed at the head-and-neck tumor board, which consists of head-and-neck surgeons, oral surgeons, dentists, interventional radiologists, and radiation oncologists. The tumor board has met weekly since the 1970s. Every new patient with head-and-neck cancer has been examined at the same institution by doctors with different expertise. After discussion, possible treatment options are presented to patients and they choose their preferred treatment. When tumor thickness approaches 1.5 cm, our treatment options can vary considerably. From the perspective of a radiation oncologists, a two plane implant is required,[1] although there is the high risk of necrosis of the mucosa and mandible. The University of Florida group reported that the incidence of severe complications were 9%.[3] Surgeons hesitate in recommending a near hemiglossectomy particularly for young patients. This is because the procedures are to some extent associated with orocutaneous fistula, flap necrosis, dysphagia, and speech disturbance.[2] Hence, treatments for tumors such as ours are controversial. In this short report, we discuss the difficulties regarding management of thick cancer of the tongue.

MATERIALS AND METHODS

From August 2003 to February 2005, 5 patients with tumor thickness close to 1.5 cm were referred to our tumor board. Tumor thickness was evaluated manually and by magnetic resonance imaging. The well known Manchester System specifies using a single plane implantation only for tumors with a thickness of less than 12 mm. If the thickness exceeds 12 mm, a two plane implantation should be implemented. Fig. 1 shows the concept of a two plane implant. As shown, full strength Cs needles are implanted at the outer edge of the tongue. It is likely that the risk of mucosal necrosis will be high. We therefore modified this implant system. According to this modification, the mucosal surface will still receive 7,000 cGy, but within the tumor there will be 1.1-1.2 times higher dose points. Fig. 2 is a representation of our modified implant. This is an ideal implantation. In reality, the outer needles were inserted up to a depth of 2-3 mm from the mucosal surface. To reduce the dose to the mandible, we used a custom-made spacer for each patient as described previously.[4] Cs implantation was carried out by T.N., and it was performed under general anesthesia in all cases. The needles' position was observed by a portable diagnostic X-ray machine, and if needed, reinsertion of a needle was performed. A nasopharyngeal airway was kept in place for a few days to prevent possible air way obstruction due to edema. Patients were examined using computed tomography (CT) to confirm good 3-dimentional needle alignment. The image was also used to measure the horizontal length of the needles for dose calculation. In both planes, the needles were inserted according to the Manchester System. The dose was prescribed at the plane 0.5 cm away from the source plane (coincidentally, this value meant that the prescribed dose was on the mucosal surface, as the tumor thickness was about 1.5 cm in all patients). The dose rate at the mucosal surface varied from 1,211 cGy/day to 1,410 cG/day with a mean dose of 1,262 cGy/day. The mean dose of the inner

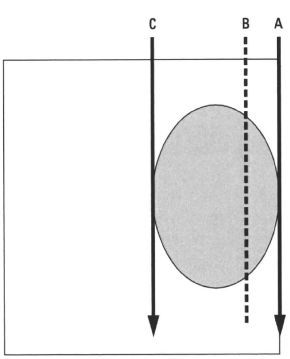

Fig. 1. Original Manchester System for T2N0 with a thickness of 1.5 cm. The tumor is shown sandwiched between full length needles. Dose is prescribed at the 0.5 cm plane B from the lateral border of the tongue. Overdose is a concern at plane A.

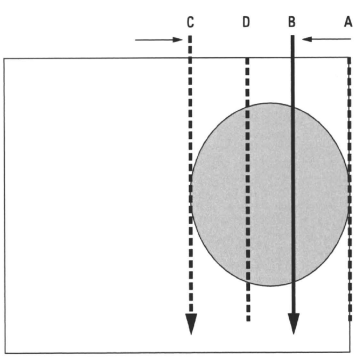

Fig. 2. Modified Manchester System at Hokkaido University. Insert full intensity needles 5 mm from the lateral border of the tongue. Half intensity needles were implanted at the medial border of the tumor. Dose is prescribed at plane A. Dose at plane D, which is 1.1 - 1.2 time higher than that at the plane A, is a concern.

plane was 1,469 cG/day with a range from 1,392 cGy/day to 1,499 cGy/day. In one patient, a needle implanted near the base of the tongue was difficult to remove, and the needle was removed under general anesthesia.

RESULTS

Table 1 shows the characteristics and outcomes of the patients. It also includes the time to be spent for insertion. One patient died from metastasis to the lung, and another patient died from metastasis to the lymphnodes. The former patient (Pt. 3) needed 2.5 hours for insertion (i.e., reinsertion was necessary to obtain an ideal configuration of needles). The patient with lymph node metastasis (Pt. 1) refused selective neck dissection because for cosmetic reasons, and developed repeated nodal metastases. Node removal was performed whenever metastasis developed. In all the patients who developed nodal recurrences, their primaries were preserved. Acute mucositis (RTOG Grade 3) subsided within one month after removal of needles in all patients and there have been no mucosal bleedings. At 6 months, all patients developed atrophy (RTOG Grade 2) of the tongue. However this did not cause any inconvenience to the patients.

Fig. 3 shows a typical case with a 1.5 cm-thick T2 tumor. The oral surgeons' recommendation was a near- hemiglossectomy. In addition, they believed that even if brachytherapy succeeded, because of the risk of nodal relapse the primary and the nodal area should be removed en bloc. This is because they think that if a primary recurs after a neck dissection, it will be almost impossible to salvage the patient. The head-and-neck surgeons had an intermediate opinion. They thought that the tumor was curable with either an operation or brachytherapy, although surgery would provide higher local control. Because of the patient's age, and the resulting undesirable cosmetic effect, disturbance in speech, swallowing, and taste, secondary to surgical intervention, brachytherapy was recommended. Radiation oncologists were a little hesitant in performing brachytherapy because of the high complication rate; however, the patient decided to be treated with brachytherapy. To minimize complications, we performed Cs implantation with the modified Manchester System mentioned above. At 2.5 years after the treatment, the patient has had no signs of complications or loco-regional recurrence.

DISCUSSION

It is well known that for carcinoma of the tongue, tumor thickness is one of the prognostic factors of regional nodal recurrence.[5,6] Our nodal recurrence rate was 60% (3/5), which is consistent with those reports. It should be noted that there has been no nodal recurrence among the 3 patients treated with selective neck dissection. There have been no reports on the relationship between Cs insertion time and outcome, but there might have been tumor cell seeding during the prolonged procedure (Pt. 3). Selective neck dissection has gradually gained popularity, and several studies have reported its efficacy.[7-10] It is unlikely that our patients will develop further recurrence in the neck, as around 90% of lymphnode relapse occurs within 1 year of the first event.[12] There has been controversy regarding how to manage a clinically controlled tongue in a patient who develops nodal disease. In our institute, although there is no definitive policy, a large primary that was initially thought to be uncontrollable by brachytherapy is a candidate for neck dissection with near-hemiglossectomy. The Kyushu University Group analyzed 396 patients who were treated with

Table 1. Patient Characteristics and Treatment Outcome

No.	Yrs	Follow-up (months)	Pathology	Thickness	Maximum distance	Local	Time to spend for Cs insertion	Complication (RTOG Grade) Early	Lete	Neck node	Present status
1	70	36	Poorly diff. SCC	1.7 cm	3.2 cm	NED	1.5 hrs	GIII	GII	7 months-ND (level I only)	died of disease
2	57	38	Moderately diff. SCC	1.6 cm	3.5 cm	NED	2 hrs	GIII	GII	5 months-ND (level II and III)	NED
3	29	24	Poorly diff. SCC	1.5 cm	3.5 cm	NED	2.5 hrs	GIII	GII	6 months-ND (level I and III)	died of lung metastasis
4	30	30	Well diff. SCC	1.5 cm	3.0 cm	NED	1.5 hrs	GIII	GII	None	NED
5	53	27	Well diff. SCC	1.6 cm	2.9 cm	NED	1 hr	GIII	GII	None	NED

ND, neck dissection; NED, no evidence of disease.

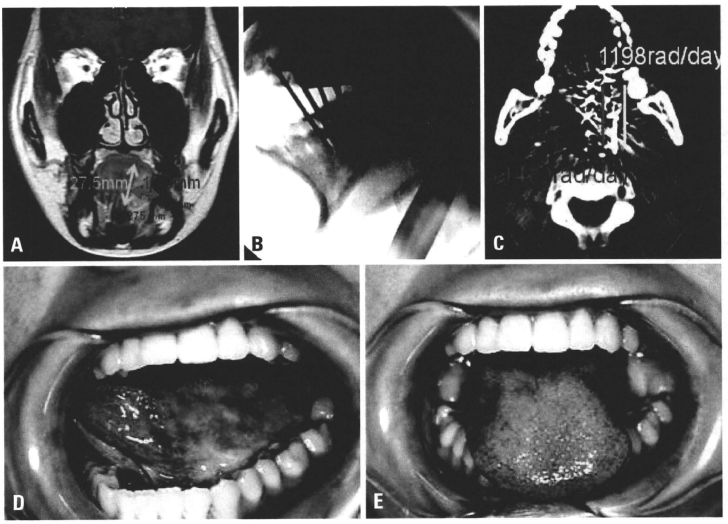

Fig. 3. (A) Gadolinium-enhanced MR image clearly revealed the tumor. The thickness was 15.3 mm and the height was 27.5 mm. (B) Operating room X-ray image. A total of 15 Cs needles were implanted. Their alignment was satisfactory. (C) CT image immediately after implant. The lateral needles were implanted 0.5 cm from the mucosal surface. The inner needles were placed 1.0 cm from the lateral needles. This alignment was the same as in the simulation. The dose prescription plane is highlighted in yellow (1,198 rad/day) and the inner plane 5 mm away from the outer needle plane is highlighted in red (1,437 rad/day). The dose at the red plane will end up with 20% higher than that of the lateral portion of the tongue. (D) Appearance of the tongue mucosa 2.5 years after the implant. The mucosa appears slightly white, there is no sign of tissue necrosis. (E) Slight atrophy is seen in the area of the implant. When the tongue protrudes, a slight deviation to the left is observed.

brachytherapy and concluded that glossectomy is unnecessary if primary sites were clinically controlled.[11] However, the number of cases with nodal dissection with glossectomy was only 6 and their T stage was not documented.

In the present study, we used magnetic resonance imaging (MRI) to measure tumor thickness. The tumor border was clearly seen in all cases. This is very helpful in making a treatment decision and also for simulating Cs implantation. The inner tumor border is sometimes ambiguous. Our current diagnostic procedures include MRI, CT, and positron emission tomography (PET). The high local control rate in this study might have been achieved because of the careful treatment planning based on these images. As to the local control rate, Hareyama, et al.[13] reported treatment results of 130 patients treated with brachytherapy. Their local control rate for T3 cases was 70.9%.[13] Since our cases were nearly T3 in terms of tumor thickness, in the sense that they needed two-plane implantation, our treatment results are comparable with theirs. The aforementioned study indicates that the overall incidence of ulceration of the tongue and mandibular complication was 20% (26/130) and 13% (17/130), respectively.[13] Although the follow-up period is still short, our patients did not show any signs of complications in soft tissues and mandibles. We would like to believe that this was due to our modified method of insertion. A multidiscipline approach is also important in deciding on a treatment plan. Previously, we reported a T4 tongue cancer that was treated with intra-arterial chemotherapy and brachytherapy using high-dose-rate (HDR) iridium.[14] The patient continues to be free from diseases and complications 7 years after treatment. To the best of our knowledge, patients being evaluated at the same time by physicians with different expertise, followed by a discussion on the best treatment plan, are rare in Japan and abroad. In many institutions, patients are simply "referred" to the radiation oncology department. The multidisciplinary approach is an established tradition in our university and it is what we want to continue in the future.

Dose heterogeneity occurs with the modified Manchester System; in other words, the outer surface receives 7,000 cGy but the inner 0.5-cm plane may receive 8,000 cGy. We initially thought that a few patients would develop a persistent mucosal ulcer. However, to our surprise, no patients developed any signs of a mucosal ulcer. This could indicate that the presence of the high dose area in deep muscle (far from the mucosa surface) does not lead to a mu-

cosal ulcer. The T4 case mentioned above also received 30 Gy external radiation and 48 Gy in 12 HDR fractions, and did not develop any signs of a mucosal ulcer. Although the number of cases is too small to discover the reason, good needle arrangement may be a factor in both local control and the absence of complications. For the past 15 years, most brachytherapy, including all 5 cases in the present report, were performed by T.N. After a discussion between the authors, H.S, and M.N. regarding the reason for the low primary control rates in T2 cancer, M.N. suggested that external radiation should be omitted, and in 1993 we changed the treatment policy to 7,000 cGy using Cs implants only. A learning curve may have also contributed to the good local control in the present series. This is not based on science, but the success of brachytherapy seems to depend on a physician's enthusiasm. Cs implants for tongue cancer are no longer available at a hospital in Manchester since the specialist for this treatment modality retired (personal communication).

In summary, although the number of patients in this series was small, the modified Manchester System resulted in good local control and no complications. Evaluation of tumor geometry by advanced diagnostic tools is important for treatment planning, and good needle alignment is essential. Increasing the number of patients treated by this technique is required to make a definitive conclusion.

ACKNOWLEDGEMENTS

This study was supported by a Grant-in-Aid for Scientific Research (B20390319), which was provided by the Ministry of Education, Science and Culture of Japan.

REFERENCES

1. Duthie MB, Gupta NK, Pointon CS. Head and neck. In: Pointon RCS, editor. The radiotherapy of malignant disease. London: Springer-Verlag; 1991. p.156.
2. Hosokawa Y, Shirato H, Nishioka T, Tsuchiya K, Chang TC, Kagei K, et al. Effect of treatment time on outcome of radiotherapy for oral tongue carcinoma. Int J Radiat Oncol Biol Phys 2003;57: 71-8.
3. Mendenhall WM, Riggs CE, Cassisi NJ. Treatment of head and neck cancers. In: Devita VT, Hellman S, Rosenberg S, editors. Cancer principle and practice of oncology. Philadelphia: Lippincott Williams and Wilkins; 2005. p.682.
4. Obinata K, Ohmori K, Tuchiya K, Nishioka T, Shirato H, Nakamura M. Clinical study of a spacer to help prevent osteoradionecrosis resulting from brachytherapy for tongue cancer. Oral Surg Oral Med Oral Pathol Oral Radiol Endod 2003;95:246-50.
5. O'Brien CJ, Lauer CS, Fredricks S, Clifford AR, McNeil EB, Bagia JS, et al. Tumor thickness influences prognosis of T1 and T2 oral cavity cancer--but what thickness? Head Neck 2003;25: 937-45.
6. Po Wing Yuen A, Lam KY, Lam LK, Ho CM, Wong A, Chow TL, et al. Prognostic factors of clinically stage I and II oral tongue carcinoma-A comparative study of stage, thickness, shape, growth pattern, invasive front malignancy grading, Martinez-Gimeno score, and pathologic features. Head Neck 2002;24:513-20.
7. Mukhija V, Gupta S, Jacobson AS, Anderson Eloy J, Genden EM. Selective neck dissection following adjuvant therapy for advanced head and neck cancer. Head Neck 2009;31:183-8.
8. Frank DK, Hu KS, Cullinev BE, Persky MS, Nussbaum M, Schantz SP, et al. Planned neck dissection after concomitant radiochemotherapy for advanced head and neck cancer. Laryngoscope 2005;115:1015-20.
9. van der Putten L, van den Broek GB, de Bree R, van den Brekel MW, Balm AJ, Hoebers FJ, et al. Effectiveness of salvage selective and modified radical neck dissection for regional pathologic lymphadenopathy after chemoradiation. Head Neck 2009. In press.
10. van der Putten L, van den Broek GB, de Bree R, van den Brekel MW, Balm AJ, Hoebers FJ, et al. Effectiveness of salvage selective and modified radical neck dissection for regional pathologic lymphadenopathy after chemoradiation. Head Neck 2009;31: 593-603.
11. Nishio M, Sakurai T, Kagami Y, Narimatsu N, Saito A, Hareyam M, et al. [Results of brachytherapy of tongue cancer.] Gan No Rinsho 1986;32:339-44.
12. Urashima Y, Nakamura K, Kunitake N, Shioyama Y, Sasaki T, Ooga S, et al. Is glossectomy necessary for late nodal metastases without clinical local recurrence after initial brachytherapy for N0 tongue cancer? A retrospective experience in 111 patients who received salvage therapy for cervical failure. Jpn J Clin Oncol 2006;36:3-6.
13. Hareyama M, Nishio M, Saito Y, Kagami Y, Asano K, Oouchi A, Narimatsu N, et al. Results of cesium needle interstitial implantation for carcinoma of the oral tongue. Int J Radiat Oncol Biol Phys 1993;25:29-34.
14. Nishioka T, Homma A, Furuta Y, Aoyama H, Suzuki F, Ohmori K, et al. A novel approach to advanced carcinoma of the tongue: cases successfully treated with combination of superselective intra-arterial chemotherapy and external/high-dose-rate interstitial radiotherapy. Jpn J Clin Oncol 2006;36:822-6.

Radiol Phys Technol (2010) 3:16–22
DOI 10.1007/s12194-009-0071-4

A parameter study of pencil beam proton dose distributions for the treatment of ocular melanoma utilizing spot scanning

Kenneth Sutherland · Satoshi Miyajima · Hiroyuki Date · Hiroki Shirato · Masayori Ishikawa · Masao Murakami · Mitsuru Yamagiwa · Paul Bolton · Toshiki Tajima

Received: 7 April 2009 / Revised: 4 August 2009 / Accepted: 4 August 2009 / Published online: 19 September 2009

Abstract The results of Monte Carlo calculated dose distributions of proton treatment of ocular melanoma are presented. An efficient spot scanning method utilizing active energy modulation, which also minimizes the number of target spots was developed. We simulated various parameter values for the particle energy spread and the pencil beam diameter in order to determine values suitable for medical treatment. We found that a 2.5-mm-diameter proton beam with a 5% Gaussian energy spread was suitable for treatment of ocular melanoma while preserving vision for the typical case that we simulated. The energy spectra and the required proton current were also calculated and are reported. The results are intended to serve as a guideline for a new class of low-cost, compact accelerators.

K. Sutherland (✉) · H. Date · H. Shirato · M. Ishikawa
Hokkaido University School of Medicine,
Kita-ku Kita 12 Jo Nishi 5 Chome,
Sapporo 060-0812, Japan
e-mail: kensuth@med.hokudai.ac.jp

K. Sutherland · S. Miyajima
Japan Science and Technology,
Motomachi 4 Chome 1 Ban 8 Go,
Kawaguchi, Saitama 332-0012, Japan

M. Yamagiwa · P. Bolton · T. Tajima
Photo-Medical Research Center, Japan Atomic Energy Agency,
Kizugawa, Kyoto 619-0215, Japan

M. Murakami
Hyogo Ion Beam Medical Center,
Shinguu Chou Hikarimiya 1-2-1,
Tatsuno, Hyogo, Japan

Keywords Proton therapy · Ocular melanoma · Monte Carlo simulation · Laser acceleration

1 Introduction

Proton beams have the potential to decrease normal tissue damage and allow dose escalation in cancer therapy, because the beam profile allows a more localized dose distribution at the tumor than do traditional X-rays. For covering the volume of a target lesion in particle therapy for cancer, two methods have been employed: passive scattering and spot scanning. In the passive scattering method, secondary neutrons from scatter foils, compensators and collimators are a possible source of secondary malignancy [1]. Spot scanning was first proposed as an alternative to passive scattering methods by Kanai et al. [2] and was further investigated by Lomax et al. [3]. Spot scanning utilizes magnetic and mechanical scanning of a pencil proton beam such that individually weighted Bragg peaks are distributed under computer control [4]. For spot scanning, there is no need for patient-specific collimators, thereby reducing the whole-body neutron dose to the patient. Another advantage is that most of the particles from the accelerator can be delivered to the patient, rather than being absorbed by collimators or compensators, and therefore this method is potentially more efficient.

In this work, we present the results of Monte Carlo simulations of proton dose distributions in which we used parameterized proton beams applied to ocular melanoma. We hope that the results of this study will serve as a guide for researchers developing proton facilities for medical treatment. We comment on the potential relevance of laser-accelerated protons [5–8] for the treatment of ocular melanoma, which requires lower proton energies than do more

deeply seated tumors, as well as relatively lower doses (fewer protons) because such tumors are typically small. However, the results should be applicable to proton therapy in general.

2 Materials and methods

2.1 Monte Carlo simulation speed improvements

Geant4 [9] version 8.0p1 was used for these simulations. Geant4 has been validated previously for medical-physics applications [10]. In order to improve the execution speed, we modified the particle navigation library following Jiang and Paganetti [11]. To improve efficiency on a PC cluster, we also developed a custom parallelization of Geant4 [12]. Simulations yield exactly the same results when running in parallel on a cluster or on a single processor as long as random-number-generator seed values are maintained and are set at the beginning of each event.

Following Jiang and Paganetti [11], four physics processes were registered in the Geant4 physics list for proton interactions: proton elastic scattering (*G4HadronElasticProcess*), proton inelastic scattering (*G4HadronInelasticProcess*), ionization (*G4hLowEnergyIonisation*) and multiple scattering (*G4MultipleScattering*). For improved efficiency, only secondary protons and neutrons were tracked. The energy from secondary electrons was deposited locally because the range was assumed to be less than 1 mm in water. The Geant4 maximum step size was limited to 1 mm.

2.2 Radiation treatment simulation software

We developed an application, which investigates the effects of the proton beam diameter and energy spread on the dose distribution. The software allows the user to open a series of DICOM CT images, and specify the target volume, one or more gantry positions and various beam characteristics. The user can also enter the particle (i.e., event) count. We chose a particle count of 1 million for this study, which we determined to be sufficient for good energy deposit distribution statistics with a reasonable processing time.

We used a series of 11 CT images of a disease-free human head with a slice thickness of 2.5 mm and a pixel spacing of 0.3125 mm. The CT pixel value (in Hounsfield units) of each voxel was used for determining the voxel material. Each material was assigned a density and a chemical composition according to the data provided by Schneider et al. [13]. The software generates files, which specify the different voxel materials and an event list containing the initial source position, direction and energy of each particle in the simulation. The dose accumulation grid had the same size and dimensions as the CT data: $512 \times 512 \times 11$; i.e., we did not subsample or smoothen the CT values.

A database of depth and lateral dose profile curves was pre-computed with the use of the Monte Carlo package *Particle and Heavy Ion Transport Code System* (PHITS) [14, 15]. This database was used by our planning software for determining the initial energy peak, energy spread and spot spacing. Depth–dose curves were computed for proton beams incident on water with energies from 30 to 250 MeV in 1-MeV increments. Four values of the Gaussian energy spread were computed: 0, 5, 10 and 15%, at a depth resolution of 0.1 mm. Lateral offset tables were computed for energies from 30 to 200 MeV in 1-MeV increments, with the use of the same energy spread values, 0, 5, 10, and 15%, and with beam diameters of 0, 1.25, 2.5, 5 and 10 mm. The tables were stored in a binary format, which minimized the time necessary for reading of the data by the planning software.

An initial weighting factor was assigned to each target spot, which was used for determining the particle count. The deepest spot (associated with the highest energy) along a beam is assigned weight 1.0. Shallower spots are then assigned weights less than 1.0 based on the pre-computed database of dose distribution curves to achieve a spread-out Bragg peak (SOBP). The target weight is then used with the total particle count for assignment of individual particle counts for each target spot. At this step, the energy spread and beam diameter are factored in by addition of small random values to the initial energy and position of each particle. In the case of the energy spread, random numbers are chosen so that the resulting particle energies have a Gaussian distribution with the specified full width at half maximum (FWHM). Another pair of random numbers is chosen to place the particle within the specified beam diameter. Particles are distributed evenly along the beam axis. The particle list is then written on a file, which is read by the simulation program.

2.3 Target spot spacing

We incorporated a spot scanning method where the beam position and direction were fixed, while target spots along the beam direction were scanned by depth variation; i.e., active energy variation for depth modulation. All beams are assumed to be parallel to each other in this simulation (Fig. 1). This method requires a rapid alteration of the proton energy.

Our software also has the ability automatically to place target spots at locations with variable spacing based on the pre-computed database of dose profile curves in water. In the case of lateral spacing, lateral fall-off curves at the

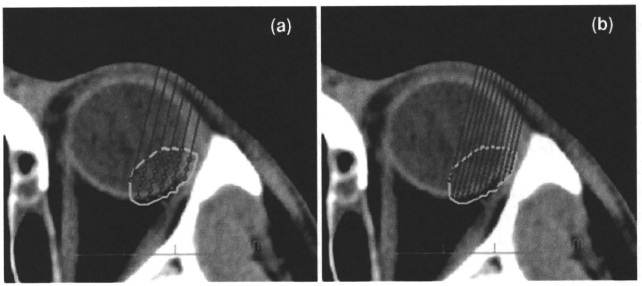

Fig. 1 Effect of beam parameters on target spot placement and beam spacing. *Blue lines* are beams. The *green polygon* is the planned target volume (PTV). *Red dots* are target spots. **a** 5-mm beam diameter and 10% energy spread. b 1.25-mm beam diameter and 0% energy spread, for which more target spots are generated (color figure online)

beam's pre-computed Bragg peak depth are used for determining the width (FWHM) of the beam, specifying a "spot width". The spot width is mostly affected by the beam diameter and by lateral scatter. For depth spacing, the beam's pre-computed depth–dose profile curve was used similarly for specifying a "spot depth". The spot depth is affected mostly by the energy spread.

Utilizing spot width and depth alone for spot spacing results in an uneven dose distribution within the target region due to under-dosed regions between spots. For achieving a smooth dose distribution, the spot width and the spot depth are multiplied by a "spacing factor". The spacing factor is usually less than 1.0 and has the effect of placing the spots closer together, i.e., increasing the number of spots. A spacing factor of 0.5, which we found yields a relatively smooth dose distribution while minimizing the number of target spots, was used throughout this simulation. A more detailed examination of the effect of the spacing factor on the dose distribution and the number of spots is a topic for future investigation.

2.4 Dose distribution optimization

It is difficult to predict the exact dose distribution in inhomogeneous patient volumes based on CT data alone. Therefore, after the initial Monte Carlo simulation, we fine-tuned the particle counts assigned to each target spot in the following way. The dose distribution for each target spot is calculated with the Monte Carlo simulation program and stored in separate files, one dose distribution file per target spot. The individual files are read and summed to form a complete dose distribution. The dose deposited at each target spot is compared with the dose average in the planning target volume (PTV). Spots that received less than the average dose (cold spots) are assigned more particles, and spots with a higher dose (hot spots) are assigned fewer particles. The process is repeated iteratively until it is determined that the result cannot be optimized further. Note that we do not attempt to reduce the dose deposited in critical structures; we only attempt to achieve a uniform dose distribution within the target volume in this optimization process.

2.5 Target polygon

The gross target volume (GTV) was modeled as a semi-ellipsoid with a semi-sphere base of height 4.8 mm and basal diameter 13 mm. The minimum tumor–optic disk distance was 5 mm. The tumor–macula distance was 4 mm. The values were chosen to represent a typical tumor based on data reported by Dendale et al. [16]. The GTV was generated in the planning software by specification of the tumor height, base diameter, eye center and tumor base position. A 2-mm margin was automatically added to the perimeter of the GTV to form the PTV. The volume of the PTV was .734 cm^3. The target polygon (PTV) and organs at risk (OARs) are shown in Fig. 2.

The prescribed dose was set to 54.5 Gy, which is equal to 60 cobalt Gray equivalent (CGE), assuming a relative radiobiological effectiveness (RBE) of 1.1. The tumor was assumed to be free of infiltration of the optic disk or macula. The dose distribution was normalized so that ninety-five percent of the PTV received at least 100% of the prescribed dose; i.e., "D95" for the PTV was set to 60 CGE. Four fractions in one week were assumed to be used, which is the common practice in conventional proton therapy. The effects of the energy spread and beam diameter were investigated with 60 CGE kept for D95 in each calculation.

3 Results

In the first series of simulations, the effect of the energy spread of the beam on the dose distribution was investigated. Energy spread values of 5, 10 and 15% were simulated. The beam diameter was 2.5 mm in each case. Dose distributions are shown in Fig. 3. Dose–volume

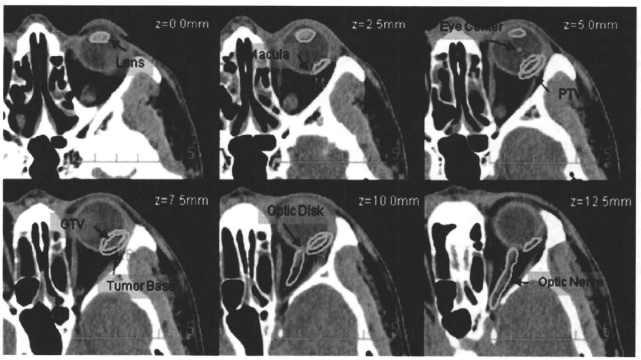

Fig. 2 Target polygons and organs at risk (OARs) used for this experiment. The inner target polygon is the *GTV*. The GTV is generated automatically by specifying the location of the tumor base and eye center. The size of the GTV is determined by specifying the basal diameter and tumor height. The outer target polygon is the *PTV* (GTV plus 2-mm margin). OARs include the lens, optic nerve macula, and optic disk (color figure online)

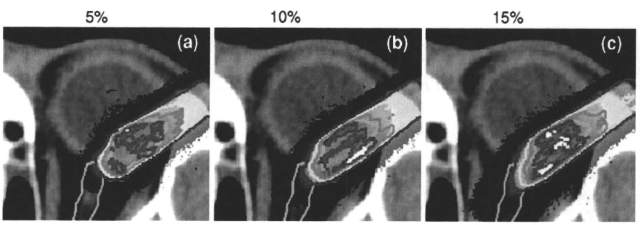

Fig. 3 Dose distributions for various values of energy spread. 5% (**a**), 10% (**b**) and 15% (**c**). Isodose lines are 125% of prescribed dose (75 CGE) *white*, 110% (66 CGE) *red*, 90% (54 CGE) *orange*, 75% (45 CGE) *yellow*, and 50% (30 CGE) *blue*. In all cases, a 2.5-mm beam width was used (color figure online)

histograms (DVHs) are shown in Fig. 4, and simulation results are summarized in Table 1. The table indicates that, at 5% energy spread, the dose to the macula and optic disc was below the tolerance values for the case that we simulated. At 10 and 15%, it was difficult to preserve critical structures located behind the distal edge of the target volume due to the elongated fall-off of the depth profile curve.

Target spot and beam characteristics are summarized in Table 2. The table shows the effect of energy spread (5, 10 and 15%) on the depth spacing and the number of target spots with a constant beam diameter (2.5 mm). The depth spacing (the distance between target spots along a beam) is increased with increasing energy spread, whereas the number of target spots is decreased with increasing energy spread.

In the second series, the effect of the beam diameter on the dose distribution was investigated. Beam diameter values of 1.25, 2.5 and 5 mm were simulated. The energy spread value for each case was 5%. Dose distributions are shown in Fig. 5, and DVHs are shown in Fig. 6. Figure 5 illustrates that the volume of hot spots in the PTV increased when the beam diameter was increased from 1.25to 2.5 mm. The simulation results are summarized in Table 3.

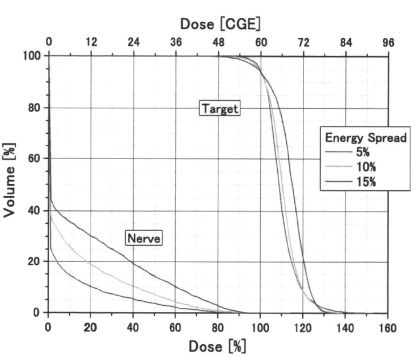

Fig. 4 DVH of PTV and optic nerve for various energy spread values. In all cases a 2.5-mm beam diameter was used (color figure online)

The table indicates that a beam diameter of less than or equal to 2.5 mm would not exceed the tolerance doses for the case that we studied. At 5-mm beam diameter, the dose to the lens becomes significant.

Table 4 indicates the effect of the beam diameter (1.25, 2.5 and 5 mm) with a fixed energy spread of 5%. The maximum and minimum values of the depth spacing were almost constant, as anticipated from the fixed energy spread. Also, the beam diameter affected the lateral spacing, as expected. The number of beams and target spots decreased significantly with an increase in the beam diameter. For a beam of 1.25 mm, nearly a thousand target spots were generated by the planning software. Such a large number of target spots would likely require a lot of time to treat.

A histogram of particle energy for a typical treatment plan is displayed in Fig. 7. In general, more particles at the higher-energy end of the spectrum are necessary because more particles are targeted at deeper locations in forming the SOBP. The energy distribution is also affected by the target shape and the incident beam direction. The energy distribution is not smooth, partly due to the discrete proton energy values used for our calculations.

Table 1 Dosimetric characteristics: energy spread

Energy spread	5%	10%	15%
Retina ≥45 CGE	1%	2%	5%
Lens ≥10 CGE	0%	0%	0%
Optic nerve ≥12 CGE	10%	20%	31%
Dose at macula (≥30 CGE)	27 (OK)	36 (NG)	42 (NG)
Dose at optic disc (≥12 CGE)	11 (OK)	1.8 (OK)	3.3 (OK)
V95[a]	98%	98%	97%

[a] Percentage volume of PTV, which received 95% of the prescribed dose (57 CGE)

Table 2 Target spot and beam characteristics: energy spread

Energy spread	5%	10%	15%
Lateral spacing (mm)	1.3	1.3	1.3
Depth spacing, minimum (mm)	0.6	1.7	3.1
Depth spacing, maximum (mm)	2.8	5.8	9.1
Number of beams	38	38	38
Number of target spots	239	102	65

Beamlet diameter was 2.5 mm for each case

4 Discussion

Many parameters and parameter combinations (such as beam diameter, energy spread, lateral spacing, depth spacing, number of beams and number of target spots) must be considered in assessing proton treatment of small superficial tumors. Realistically, some of the parameters may need to be predetermined in the clinical equipment because of mechanical or other limitations. In this study, we simulated the effect of energy spread by using a fixed beam diameter (2.5 mm), and the effect of the beam diameter by using a fixed energy spread (5%). These values were chosen because they seemed to be the most likely parameters delivered by an actual accelerator. A more thorough parameter survey is necessary for determination of the effects of every possible combination of beam parameters.

For reducing treatment times, it is desirable to reduce the number of target spots in a plan. However, there is a trade-off between the dose distribution and the number of target spots. Our results suggest that, if the beam energy and lateral spacing are predetermined, the energy spread and beam diameters must be chosen carefully with this in mind. The clinical significance of dose–volume statistics of the PTV and organs at risk must be determined for each patient.

The dose distributions shown here contain many hot spots (overdose areas). These are caused partially by the histogram normalization method, where 95% of the target volume is forced to receive at least 100% of the prescribed dose. Without normalization, cold spots were prevalent around the lateral and distal edges, especially when a large beam diameter or energy spread was used. The cold spots became prevalent when the distance from the tumor polygon edge and nearest target spot was relatively large. This resulted in DVH curves for the target volume not being as steep (selective) as they should have been. Several methods can be employed for improving the dose distributions,

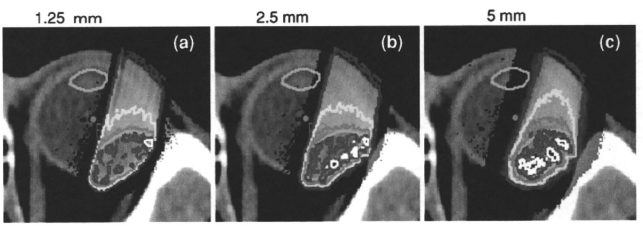

Fig. 5 Dose distribution for various values for beam diameter, 1.25 mm (**a**) 2.5 mm (**b**), and 5 mm (**c**). Isodose lines are 125% of prescribed dose (75 CGE) *white*, 110% (66 CGE) *red*, 90% (54 CGE) *orange*, 75% (45 CGE) *yellow* and 50% (30 CGE) *blue*. In all cases, we used 5% energy spread (color figure online)

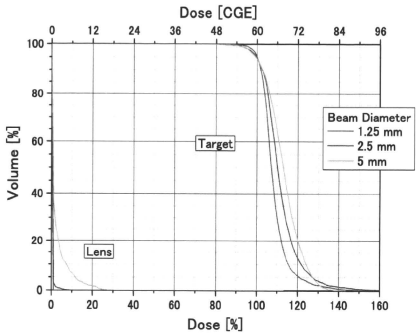

Fig. 6 DVH for PTV and optic nerve computed with various values for beam diameter. In all cases, we used 5% energy spread (color figure online)

Table 3 Dosimetric characteristics: beam diameter

Beam diameter	1.25 mm	2.5 mm	5 mm
Retina ≥45 CGE	0%	0%	1%
Lens ≥10 CGE	0%	0%	6%
Optic nerve ≥12 CGE	0%	1%	4%
Dose at macula (≥30 CGE)	13 (OK)	13 (OK)	36 (NG)
Dose at optic disc (≥12 CGE)	0.8 (OK)	3.0 (OK)	18 (NG)
V95[a]	99%	98%	98%

[a] Percentage volume of CTV, which received 95% of the prescribed dose (57 CGE)

Table 4 Spot and beam characteristics: beam diameter

Beam diameter	1.25 mm	2.5 mm	5 mm
Lateral spacing (mm)	0.7	1.4	2.6
Depth spacing, minimum (mm)	0.7	0.7	0.6
Depth spacing, maximum (mm)	2.4	2.4	2.3
Number of beams	206	57	21
Number of target spots	918	233	87

Energy spread was 5% for each case

including increasing the number of Monte Carlo events, decreasing the space between target spots and improving the optimization algorithm. Furthermore, we used a fixed spacing factor of 0.5 in this study. Introduction of a variable spacing factor for each beam may further improve the homogeneity of dose distributions. The spacing factor should be smaller near the polygon edges to prevent cold spots while maintaining a reasonable total number of spots. These are topics for future study.

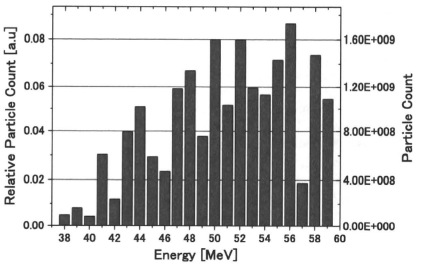

Fig. 7 A typical histogram of particle energy levels (color figure online)

In this work, doses to the macula and to the optic disc were high and above the clinical limits in some cases. This is mainly because these structures are located directly behind the distal edge of the target volume. Proton spectra that are closer to being monoenergetic may improve the final clinical outcome. The effect of energy spread for deep-seated tumors such as prostate cancer may be different from that for shallow ocular diseases and is yet to be determined.

The required proton flux can be estimated as follows. Consider a shallow tumor volume of 1 cc (1 g). If the protons deposit an average energy of 50 MeV, then each proton delivers about 8×10^{-12} J or 8×10^{-9} Gy on average. Assuming an RBE of 1.1, each proton delivers about 9×10^{-9} CGE. A typical treatment course consists of 60 CGE delivered in four fractions on consecutive days. If the irradiation time is limited to 1 min, then the accelerator must deliver 15 CGE per min or .25 CGE per s. The accelerator must therefore produce about 30 million protons per second or 4.8 pA. If such a delivery was carried out in 100 Hz repetitive pulsed laser shots, the required delivery would be in the order of 3×10^5 protons per shot.

5 Conclusion

Our simulations show that a 2.5-mm beam diameter and a 5% energy spread can be considered as a starting point for ocular cases. The dose distributions suggest that there is merit in continuing such parameter studies and considering further the potential for spot scanning proton sources.

Acknowledgments This work was supported by the Core Research for Evolutional Science and Technology (CREST), the Japan Science and Technology Agency (JST) and the Special Coordination Fund (SCF) for Promoting Science and Technology commissioned by the Ministry of Education, Culture, Sports, Science and Technology (MEXT) of Japan. K. S. is a Takuma Scholar of PMRC.

References

1. Brenner DJ, Hall EJ. Secondary neutrons in clinical proton radiotherapy: a charged issue. Radiat Oncol. 2008;86(2):165–70.
2. Kanai T, Kawachi K, Kumamoto Y, Ogawa H, Yamada Y, Matsuzawa H. Spot scanning system for proton radiotherapy. Med Phys. 1980;7(4):365–9.
3. Lomax AJ, Bohringer T, Bolsi A, Coray D, Emert F, Goitein G, et al. Treatment planning and verification of proton therapy using spot scanning: initial experiences. Med Phys. 2004;31(11):3150–7.
4. Lomax AJ, Boehringer T, Coray A, Egger E, Goitein G, Grossmann M, et al. Intensity-modulated proton therapy: a clinical example. Med Phys. 2000;28(3):317–24.
5. Tajima T. Prospect for compact medical laser accelerators. J Jpn Soc Therap Radiat Oncol. 1997;9(Suppl 2):83–5.
6. Malka V, Sven F, Lefebvre E, d'Humieres E, Ferrand R. Practicability of proton therapy using compact laser systems. Med Phys. 2004;31(6):1587–92.
7. Ma CM, Maughan RL. Point/counterpoint: within the next decade conventional cyclotrons for proton radiotherapy will become obsolete and replaced by far less expensive machines using compact laser systems for the acceleration of the protons. Med Phys. 2006;33(3):571–3.
8. Bulanov SV, Esirkepov T, Khoroshkov VS, Kuznetsov AV, Pegoraro F. Oncological hadrontherapy with laser ion accelerators. Phys Lett A. 2002;299:240–7.
9. Agostinelli S, Allisonas J, Amakoe K, Apostolakisa J, Araujo H, et al. Geant4–a simulation toolkit. Nucl Instrum Methods Phys Res A. 2003;506:250–303.
10. Carrier J, Archambault L, Beaulieu L, Roy R. Validation of Geant4, an object-oriented Monte Carlo toolkit, for simulations in medical physics. Med Phys. 2004;31(3):484–92.
11. Jiang H, Paganetti H. Adaptation of Geant4 to Monte Carlo dose calculations based on CT data. Med Phys. 2004;31(10):2811–8.
12. Sutherland K, Miyajima S, Date H. A simple parallelization of Geant4 on a PC cluster with static scheduling for dose calculations. First European workshop on Monte Carlo treatment planning, Journal of Physics: Conference Series. 2007; 74 012020.
13. Schneider W, Bortfeld T, Schlegel W. Correlation between CT numbers and tissue parameters needed for Monte Carlo simulations of clinical dose distributions. Phys Med Biol. 2000;45:459–78.
14. Iwase H, Niita K, Nakamura T. Development of a general-purpose particle and heavy ion transport Monte Carlo code. J Nucl Sci Technol. 2002;39(11):1142–51.
15. Niita K, Sato T, Iwase H, Nose H, Nakashima H, Sihver L. PHITS: a particle and heavy ion transport code system. Radiat Meas. 2006;41:1080–90.
16. Dendale R, et al. Proton beam radiotherapy for uveal melanoma: results of Curie Institute-Orsay Proton Therapy Center (ICPO). Int J Radiat Oncol Biol Phys. 2006;65(3):780–7.

ELSEVIER

Int. J. Radiation Oncology Biol. Phys., Vol. 77, No. 2, pp. 630–636, 2010

0360-3016/$–see front matter

doi:10.1016/j.ijrobp.2009.08.060

PHYSICS CONTRIBUTION

EVALUATION OF THE EFFECTIVENESS OF THE STEREOTACTIC BODY FRAME IN REDUCING RESPIRATORY INTRAFRACTIONAL ORGAN MOTION USING THE REAL-TIME TUMOR-TRACKING RADIOTHERAPY SYSTEM

GERARD BENGUA, PH.D.,* MASAYORI ISHIKAWA, PH.D.,* KENNETH SUTHERLAND,* KENJI HORITA, R.T,† RIE YAMAZAKI, R.T.,† KATSUHISA FUJITA, R.T.,† RIKIYA ONIMARU, M.D.,‡ NORIWO KATOH, M.D.,‡ TETSUYA INOUE, M.D.,‡ SHUNSUKE ONODERA, M.D.,‡ AND HIROKI SHIRATO, M.D.‡

From the *Department of Medical Physics, †Radiology Department, and ‡Graduate School of Medicine, Hokkaido University, Sapporo, Hokkaido, Japan

Purpose: To evaluate the effectiveness of the stereotactic body frame (SBF), with or without a diaphragm press or a breathing cycle monitoring device (Abches), in controlling the range of lung tumor motion, by tracking the real-time position of fiducial markers.

Methods and Materials: The trajectories of gold markers in the lung were tracked with the real-time tumor-tracking radiotherapy system. The SBF was used for patient immobilization and the diaphragm press and Abches were used to actively control breathing and for self-controlled respiration, respectively. Tracking was performed in five setups, with and without immobilization and respiration control. The results were evaluated using the effective range, which was defined as the range that includes 95% of all the recorded marker positions in each setup.

Results: The SBF, with or without a diaphragm press or Abches, did not yield effective ranges of marker motion which were significantly different from setups that did not use these materials. The differences in the effective marker ranges in the upper lobes for all the patient setups were less than 1mm. Larger effective ranges were obtained for the markers in the middle or lower lobes.

Conclusion: The effectiveness of controlling respiratory-induced organ motion by using the SBF+diaphragm press or SBF + Abches patient setups were highly dependent on the individual patient reaction to the use of these materials and the location of the markers. They may be considered for lung tumors in the lower lobes, but are not necessary for tumors in the upper lobes. © **2010 Elsevier Inc.**

Organ motion, Body frame, Real-time tracking, Effective range.

INTRODUCTION

The risk of radiation-induced lung complications may be minimized if intrafractional tumor motion caused by respiration during irradiation can be accurately accounted for. Various approaches to the management of respiratory motion in radiation therapy are comprehensively discussed in the American Association of Physicists in Medicine (AAPM) Report 91 (1). These include the accurate tracking of organ and tumor motion during treatment and methods by which the motion may be restricted or dampened.

Motion tracking may be accomplished by taking two sets of fluoroscopic images of the tumor itself, other anatomical structures, or fiducial markers placed near the tumor (2–4). Ideally, the function of real-time tracking is to determine the full range of tumor motion, as well as its trajectory during treatment from these fluoroscopic images taken at high frequency. At present, this is only possible in a few centers that have facilities dedicated for this purpose, such as the real-time tumor-tracking radiation therapy system developed at Hokkaido University Hospital (5, 6).

Restriction of respiration, on the other hand, can be achieved by using patient immobilization and by applying abdominal pressure. In extracranial stereotactic irradiation, Lax *et al.* (7), Herfarth *et al.* (8), and Negoro *et al.* (9) have reported the effectiveness of an abdominal press in reducing respiratory-induced tumor movement in stereotactic conformal radiation therapy of body tumors. Alternatively, an

Reprint requests to: Gerard Bengua, Department of Medical Physics, Hokkaido University Hospital, North-15 West-7, Kita-ku, Sapporo, 060-8648, Japan. Tel: (+81) 11-706-7638; Fax: (+81) 11-706-7639; E-mail: gerard@med.hokudai.ac.jp

The physics part of this study was supported by the grant-in-aid from the Japanese Ministry of Education, Culture, Sports, Science and Technology; the clinical portion was supported by the grant-in-aid from the Japanese Ministry of Health and Welfare.

Conflict of interest: This study was conducted in cooperation with Elekta Oncology Systems, Japan.

Acknowledgment—The authors express their gratitude to Drs. Shinichi Shimizu, Hiroshi Taguchi, and Mylin Torres for their help with the clinical aspects of this study.

Received Feb 18, 2009, and in revised form Aug 3, 2009. Accepted for publication Aug 19, 2009.